Available online at www.sciencedirect.com
SCIENCE DIRECT®
International Journal of Mass Spectrometry 245 (2005) 26–35
International Journal of Mass Spectrometry
www.elsevier.com/locate/ijms

Cross sections for ionization of Mo and Mo^+ by electron impact

Duck-Hee Kwon[a], Yong-Joo Rhee[a], Yong-Ki Kim[b,*]

[a] *Korea Atomic Energy Research Institute, Daejeon 305-600, Republic of Korea*
[b] *National Institute of Standards and Technology, 100 Bureau Drive, Gaithersburg, MD 20899-8422, USA*

Received 27 April 2005; received in revised form 17 June 2005; accepted 17 June 2005
Available online 26 July 2005

Abstract

Theoretical cross sections for electron-impact ionization of the neutral Mo atom and Mo^+ ion are reported. Both Mo and Mo^+ have many metastable levels near the ground level. We calculated ionization cross sections from the ground and two lowest metastable levels for both Mo and Mo^+. The total ionization cross sections for each initial state consist of direct and indirect ionization cross sections. The direct ionization cross sections were calculated by using the binary-encounter Bethe (BEB) model. The indirect ionization cross sections resulting from numerous excitation–autoionization processes were calculated by using scaled Born cross sections for the excitation of 5s electrons to 5p, 4d electrons to 5p, and 4p electrons to 4d or 5s, whose excitation energies exceeded the lowest ionization energy of the initial states of Mo and Mo^+. For the ground-state Mo, indirect processes contribute only about 5%, while for metastable Mo, indirect processes contribute almost 30% to the total ionization cross section. Unlike our experience with light atoms, contributions to indirect ionization from spin-forbidden and $\Delta n = 1$ excitations, where n is the principal quantum number, are noticeable. For Mo^+ indirect processes contribute less than 15%. There are no experimental data to compare for Mo. The distorted-wave Born cross sections for Mo available in the literature accounted for direct ionization only, and hence are lower than in the present work at higher incident electron energies where excitation–autoionization contributes significantly. Our total cross section for the single ionization of Mo^+ is in good agreement with two sets of experimental data available in the literature, while the distorted-wave Born cross section reported with one of the experiments is almost a factor of two higher than the experiments at the cross section peak.

Keywords: Ionization cross sections; Mo and Mo^+; Autoioniztion

1. Introduction

Molybdenum and tungsten are refractory metals which have desirable properties to line the inside of magnetic fusion devices such as tokamaks. In fact, Massachusetts Institute of Technology has a working tokamak whose inside is lined with molybdenum tiles. In the 1970s, modeling studies indicated that lining the inside wall of a tokamak with heavy metals such as tungsten would lead to severe loss of plasma energy through collisional excitations of metal ions in the plasma by plasma electrons and subsequent radiative decay of the excited metal ions. The emitted photons not only will cool the plasma and prevent it from ignition, but also they will be absorbed into the wall and release more impurity atoms into the plasma. However, a recent trend is to reconsider this pessimistic scenario. Tungsten is being introduced into large tokamaks in Germany and Japan, primarily in the divertor region, and tungsten will also be used in the International Thermonuclear Experimental Reactor (ITER). We have applied a set of theoretical procedures described below to calculate total ionization cross sections of Mo and Mo^+ not only to demonstrate the validity of our method, but also in preparation for calculating similar ionization cross sections for tungsten.

The valence shell structure of Mo (atomic number $Z = 42$) is $4d^5 5s$. Contributions to total ionization cross sec-

* Corresponding author. Tel.: +1 301 975 3203; fax: +1 301 975 3038.
E-mail address: kim@nist.gov (Y.-K. Kim).

1387-3806/$ – see front matter © 2005 Elsevier B.V. All rights reserved.
doi:10.1016/j.ijms.2005.06.007

tions of atoms with open valence configurations consists of two major components, direct ionization of bound electrons into the continuum and indirect ionization through excitation of inner-shell electrons to excited "bound" levels followed by autoionization which is called excitation–autoionization (EA). Hence, theoretical calculation of total ionization cross sections of atoms must include both direct ionization and EA processes. The main objectives of the present work are to provide reliable total ionisation cross sections of Mo and Mo^+ by electron impact and identify the type of transitions that contribute significantly to EA as the atomic number increases. For this purpose, we use the binary-encounter Bethe (BEB) model for direct ionization [1] and scaled Born cross sections for EA [2,3] to calculate total ionization cross sections of Mo and Mo^+ ions. Relativistic wave functions are used to calculate all cross sections. The same theoretical procedure has successfully been applied to neutral B (atomic number $Z = 5$), C ($Z = 6$), N ($Z = 7$), O ($Z = 8$), Al ($Z = 13$), Ga ($Z = 31$), and In ($Z = 49$) [4,5]. The atoms in column IIIB of the periodic table (B, Al, Ga, and In) have simple valence configuration (ns^2np), and autoionizing terms with the configuration $nsnp^2$ accounted for almost one-half of total ionization cross sections [4]. On the other hand, EA of the second-row atoms (C, N, and O) amounted to less than 20% of the total ionization cross section.

Among these atoms, only N has a half-filled valence configuration ($2p^3$) as in the case of Mo ($4d^55s$) and Mo^+ ($4d^5$). Unlike the case of N, however, the valence configurations of Mo/Mo^+ produce numerous metastable levels spread across the entire spectrum of bound levels. There is no guarantee that the theoretical methods that worked well for light open-shell atoms such as C, N, and O would work equally well for heavy atoms such as Mo and W, which have much more complex valence configurations. For instance, relativistic effects will become increasingly visible, most notably through intermediate coupling that will make spin quantum numbers less important in identifying strong excitations that lead to autoionization. For the light atoms reported in [5], only a few autoionizing excited levels contributed significantly to total ionization cross sections. For Mo/Mo^+, there are literally thousands of autoionizing excited levels. Although most of these autoionizing levels have small excitation cross sections, is it safe for us to include only $\Delta n = 0$, electric dipole ($E1$)- and spin-allowed excitations, as we did for the light atoms?

Another notable feature observed in light atoms was that the total ionization cross sections of two metastable N ($2p^3\ ^2D$ and ^2P) were very close except in the vicinity of their thresholds [5]. Can we safely assume that all or most metastable Mo/Mo^+ also would have similar cross sections? Ionization cross sections for metastable N were higher than the cross section for the ground level N primarily because the binding energies were lower for the metastable N. Can we assume the same trend for metastable Mo/Mo^+? The autoionizing levels are inherently unstable, and hence most of their wave functions cannot easily be made fully self-consistent even if we treat them as isolated bound levels. The only practical way to calculate thousands of such wave functions is to generate radial functions from configuration average, freeze them, and then construct the angular part to be eigenfunctions of appropriate J. Will such wave functions produce useful results when thousands of levels are involved? Also, this is the first time we have applied the combination of the BEB model and scaled Born cross sections to an atomic ion. These are some of the important questions that must be studied before we can safely extend the present combination of theoretical methods to heavy atoms with complex valence structures. In particular, the issue of identifying significant EA contributions poses a serious challenge to theorists because there are no *reliable* way at present to calculate cross sections for excitations to such autoionizing levels directly from the Schrödinger equation.

Because of the low vapor pressure of Mo, there are no experimental data on electron-impact ionization of the neutral Mo atom to compare to theory. However, there are experimental data on the ionization of Mo^+, which can be used to judge the reliability of the present work. Since we use the same theoretical models for Mo and Mo^+, good agreement with experiments on Mo^+ should provide confidence in the reliability of our results on Mo.

Available experimental data [6,7] for Mo^+ show the appearance of Mo^{2+} ions at incident electron energies several eV below the ionization energy (IE) of the ground level Mo^+ (16.15 eV), clearly indicating that the experimental target beams contained a substantial fraction of metastable Mo^+ ions. Since the plasma conditions in fusion devices are expected to be different from the conditions under which these experimental target ions were generated, fusion plasma modelers will need ionization cross sections for the ground level and metastable levels separately so that the modelers can try different mixtures to emulate fusion plasma conditions. On the other hand, it is impractical to calculate ionization cross sections for every metastable level because there are too many of them. According to our prior experience [5], metastable levels similar in excitation energies, such as the members of a fine-structure multiplet, have almost identical cross sections.

For both Mo and Mo^+, theoretical ionization cross sections based on the distorted-wave Born approximation (DWBA) have been published [7,8]. The DWBA cross section for the ionization of Mo^+ [7] is almost twice as large as the experiments at the peak. Our goal in the present work is to demonstrate that a combination of practical theoretical methods can produce total ionization cross sections that are reliable to $\pm 15\%$ or better at the peak, and have good agreement in overall shape with known experimental results from the threshold to a few keV in the incident electron energy. At the same time, we hope to answer the questions raised earlier and pave the ground work to apply our theory to heavy atoms such as tungsten. The theory used is briefly described in Section 2, the calculation for Mo^+ is described in Section

3, that for Mo in Section 4, and the conclusions are stated in Section 5.

2. Outline of theory

The largest contribution to ionization usually comes from direct ionization, i.e., ejection of a bound electron directly into the continuum. Among the many indirect ionization processes, the most prominent one is excitation–autoionization (EA) as was mentioned in Section 1. For light atoms (C, N, O in [5]) and atoms with simple valence configurations (B, Al, Ga, In in [4]) we found that it was sufficient to use only $\Delta n = 0$, $E1$- and spin-allowed excitations to estimate cross sections for EA. In contrast, with increased relativistic effects and smaller energy gaps between loosely bound orbitals in Mo and Mo^+, we expect that noticeable contributions may also come from $\Delta n = 1$ and $E1$-allowed ($\Delta J = 0, \pm 1$) but spin-forbidden excitations. One notable advantage of the theoretical models described below is that they are capable of using cross sections obtained from relativistic and nonrelativistic wave functions without any significant modifications unlike more rigorous theories such as the R-matrix theory.

2.1. Binary encounter Bethe (BEB) model for direct ionization

The BEB model [1] combines the asymptotic form of the plane-wave Born (PWB) cross section with a modified form of the Mott cross section without using any empirical parameters. The BEB model provides the ionization cross section σ_{nl} for each atomic orbital (n = principal quantum number; l = orbital angular momentum) using the orbital binding energy B, kinetic energy U, electron occupation number N, and the incident electron energy T:

$$\sigma_{nl} = \frac{4\pi a_0^2 N R^2}{B^2(t+u+1)} \left[\frac{\ln t}{2} \left(1 - \frac{1}{t^2} \right) + 1 - \frac{1}{t} - \frac{\ln t}{t+1} \right], \tag{1}$$

where a_0 is the Bohr radius and R is the rydberg energy, $t = T/B$ and $u = U/B$. The total direct ionization cross section is obtained by summing σ_{nl} over all occupied orbitals. Eq. (1) has produced cross sections in good agreement with accurate theories and experiments for light atoms and dozens of molecules.

Although both the PWB and Mott cross sections originated from rigorous applications of Schrödinger equations, the BEB model itself is not a solution of any specific Schrödinger equation. In particular, the denominator, $t + u + 1$, is a modification of the original PWB and Mott cross sections to emulate the strong correlation between the incident and target electrons at low T. Most collision theories, including the original PWB and Mott cross sections, have only t in the denominator. Minor modifications to this denominator were introduced to apply the BEB model to orbitals with $n > 2$ in heavy neutral atoms such as Mo:

$$\sigma_{\text{neut}} = \frac{4\pi a_0^2 N R^2}{B^2[t + (u+1)/n]} \times \left[\frac{\ln t}{2} \left(1 - \frac{1}{t^2} \right) + 1 - \frac{1}{t} - \frac{\ln t}{t+1} \right], \tag{2}$$

and for their singly charged ions, such as Mo^+:

$$\sigma_{+} = \frac{4\pi a_0^2 N R^2}{B^2[t + (u+1)/2n]} \times \left[\frac{\ln t}{2} \left(1 - \frac{1}{t^2} \right) + 1 - \frac{1}{t} - \frac{\ln t}{t+1} \right]. \tag{3}$$

These modifications were introduced to avoid unrealistically small cross sections resulting from increasing values of U as n increases in heavy atoms. The introduction of the factor 2 in the denominator of Eq. (3) reflects the fact that the original Mott cross section with only t in the denominator will eventually become accurate for highly charged ion targets. Both modifications have successfully been applied to molecules and molecular ions that contain heavy atoms [9].

Note that Eqs. (1)–(3) require data only from the initial bound states, which are far easier to calculate than properties that directly involve continuum states. The orbital constants B, U and N can be obtained from nonrelativistic or relativistic wave functions, although the latter is preferred for heavy atoms as we did for Mo and Mo^+. Eqs. (1)–(3) are based on nonrelativistic theories and hence valid only for nonrelativistic T.

2.2. Scaled born cross sections for excitation

The PWB cross section for the excitation of a neutral atom and the Coulomb Born (CB) cross section for the excitation of an ion are both based on the first-order perturbation theory, and hence share the same shortcoming, i.e., they are reliable only at high T. It was found earlier that simple scalings, to be referred to as *BE scaling* for PWB cross sections [2] and *E scaling* for CB cross sections [3], can be used to modify these Born cross sections at low T so that they become reliable at all T. These scalings are valid only for $E1$-*allowed, strong* excitations:

$$\sigma_{BE} = \sigma_{\text{PWB}} \frac{T}{T + B + E}, \tag{4}$$

where E is the excitation energy, and

$$\sigma_{E} = \sigma_{\text{CB}} \frac{T}{T + E}. \tag{5}$$

Both the *BE* scaling and *E* scaling have been verified to produce reliable results at low T for light as well as heavy atoms [2,3]. These scaling methods can be used for excitations to both low-lying (hence true bound) levels as well as highly excited (i.e., autoionizing) levels. These scalings cannot be used on weak processes such as $E1$-forbidden excitations because cross sections for such weak transitions cannot

be accurately described by the first-order Born approximation, particularly at low T.

2.3. Atomic structure of Mo and Mo^+

It is adequate to use LS coupling for Mo and Mo^+ to identify their energy level structures because their fine-structure multiplets are well separated from each other. However, selection rules based on LS coupling may not be adequate to identify strong excitations contributing to autoionization because intermediate coupling may become important as was mentioned earlier. To calculate transition rates and excitation cross sections using relativistic selection rules, we used two versions of the relativistic codes primarily developed by Desclaux and Indelicato [10]. We shall simply refer to them as the old and new MCDF (multiconfiguration Dirac–Fock) codes.

For the neutral Mo atom the new MCDF code provides all necessary theoretical data, i.e., orbital constants B, U, and N of the initial state, ground and excited energy level data with the usual L, S, J quantum numbers and the parity, and PWB cross sections for electron-impact excitations to be used for EA. The orbital constants to be used in Eqs. (1)–(3) need not be very accurate, except for the lowest binding energy B of the valence orbital. The lowest B must be accurate to compare the cross sections near the ionization threshold with available experimental data. The energy levels and IEs (=the lowest binding energies B) of neutral Mo and its ions are known [11] and we used them for both Mo and Mo^+. We used values obtained from the new MCDF code for other orbital constants. The old set of codes do not identify the L, S and J quantum numbers of energy levels and the computational procedures are slower than the new codes. However, only the old codes provide the CB excitation cross sections required for Mo^+.

Correlated wave functions are not always helpful because the interpretation of the binding energy B of the correlation orbitals which are not normally occupied (such as 5p or 4f orbitals in the ground state of Mo) may cause confusion as to which electron is being ionised to produce the desired ion. For this reason, we chose wave functions with (nonrelativistically) single configurations for the initial states. Also, our experience indicates that the BEB cross sections calculated from correlated, fully self-consistent wave functions are very close to those calculated from uncorrelated wave functions [5].

For both Mo and Mo^+, we have searched for significant autoionizing excitations by limiting to those involving $5s \rightarrow 5p$, $4d \rightarrow 5p$, $4d \rightarrow 4f$, $4p \rightarrow 4d$, and $4p \rightarrow 5s$ excitations because they are likely to have large cross sections. Even with this simplification, there are hundreds of $E1$-allowed excitations. We chose only those with the $E1$ oscillator strength $f > 0.05$.

To identify significant autoionizing excitations, we need to know both their excitation energies from the initial state and cross sections. Since configuration mixing is significant for the excited states of open-shell atoms such as Mo and Mo^+, we mixed singly and doubly excited configurations involving 4p, 4d, 4f, 5s, and 5p orbitals. The radial functions were calculated in the configuration average, i.e., without specifying J. Then, these radial functions were kept frozen while the angular functions were coupled through jj coupling to generate the desired eigenfunctions of J^2. The new MCDF code identifies the leading L, S, and J quantum numbers of each level, and hence we are able to confirm that some of the excitations with $f > 0.05$ are spin-forbidden. In contrast, autoionizing excitations with $f > 0.05$ for C, N, and O reported in [5] were all spin-allowed.

The individual excitation energies produced from these wave functions with frozen orbitals are not reliable by themselves. To obtain more realistic excitation energy E to be used in Eqs. (4) and (5), we multiplied the ratio of the calculated and experimental IEs to the theoretical excitation energies.

3. Cross sections for Mo^+

3.1. Direct ionization

The direct ionization cross section of Mo^+ was calculated using Eq. (3). The orbital parameters for the ground level ($4d^5\ ^6S_{5/2}$) and two metastable levels ($4d^4 5s\ ^6D_{5/2}$ and $4d^5\ ^4G_{5/2}$) are listed in Table A.1.

Among the many metastable levels of Mo^+, we chose the $4d^4 5s\ ^6D_{5/2}$ level (1.540 eV above the ground level) and the $4d^5 {}^4G_{5/2}$ (1.884 eV above the ground level) because (a) they are the first and the second metastable terms, (b) cross sections for the levels in a given term are very close as we mentioned earlier, and (c) keeping the same J as the ground level simplifies some computational steps.

In the case of the ground level ($4d^5 {}^6S_{5/2}$) and the second metastable level ($4d^5 {}^4G_{5/2}$), one of the 4d electrons is ionized with the experimental IE of 16.15 eV and $16.15 - 1.884 = 14.266$ eV, respectively, while for the first metastable level ($4d^4 5s {}^6D_{5/2}$) the 5s electron is ionized with the experimental IE of $16.15 - 1.540 = 14.610$ eV. In all cases, the resulting Mo^{2+} ion is in its ground term ($4d^4\ ^5D$) or in one of the many metastable terms with the same configuration. We have assumed the Mo^{2+} ions are statistically distributed in the five levels of the ^5D ground term. The center of gravity (c.g.) of the ^5D term is 0.1462 eV above the ground level $^5D_0$. We added this c.g. energy to the known IE of Mo^+, making the IE we used $16.15 + 0.1462 = 16.2962$ eV. We also added 0.1462 eV to the IEs of the two metastable Mo^+ levels.

The Mo^{2+} ions produced are most likely to have the configuration $4d^4$ regardless of the initial state of Mo^+. Of the numerous metastable Mo^{2+} terms with the $4d^4$ configuration, the lowest four terms are about 1.4–2.07 eV above the ground level, which are comparable to the excitation energies of the low-lying Mo^+ metastable levels. Hence, the effective IEs of the Mo^+ metastable levels resulting in metastable Mo^{2+} are similar to the IE of the Mo^+ ground level resulting in the ground term of Mo^{2+}. The IEs for producing metastable

Mo^{2+} from the Mo^{+} ground level would require IEs exceeding 17 eV. The experimental data in Fig. 1 start to rise from $T \sim 14$ eV, an indication that many of the incident Mo^{+} ions used in the experiments were metastable, and the resulting Mo^{2+} ions were likely to have been in the ground term of Mo^{2+}. The BEB cross sections for the direct ionization of the ground and the metastable levels of Mo^{+} all producing Mo^{2+} in its ground term is listed in Table A.2.

3.2. Indirect ionization

Unlike the case of the second and third row atoms, nothing is known about the autoionizing levels of Mo^{+}, although it is certain that the ion must have many. Hence, we must estimate the contribution to indirect ionization by EA solely from theory. Our computer codes reach their limits quickly in terms of the configurations they can incorporate and the accuracy they can achieve for an atom with as complex structure as Mo and Mo^{+}. Hence, we had to use simpler theoretical procedures than the ones we have used for light atoms.

As stated earlier, we have used configuration average radial functions to construct wave functions for the excited states whose excitation energies exceed the IE of the 4d electron (for the ground level) and the 5s electron (for the metastable levels). We have retained only $E1$-allowed excitations whose f values exceeded 0.05. Out of hundreds of excitations representing 5s → 5p, 4p → 4d, 5s, and 4d → 4f, 5p excitations, we found none of the excitations to 4f and 5p satisfied the f-size criterion, while there were 14 qualifying excitations of the 4p electrons in the ground level, 12 excitations of the 4p electrons in the $^6D_{5/2}$ metastable level, and 11 excitations of the 4p electrons in the $^4G_{5/2}$ metastable level. Among these, a total of 10 excitations were very strong ($f > 0.2$), and two of them were $\Delta n = 1$ (4p → 5s) excitations while one of them was a spin-forbidden transition with an f value of 0.73. A similar breakdown of LS coupling is also observed in the resonance transitions in Kr, in which the f values for the $4p^6\,{}^1S_0 \rightarrow 4p^5 5s\ {}^3P_1$ and $4p^6\,{}^1S_0 \rightarrow 4p^5 5s\ {}^1P_1$ excitations are 0.214 ± 0.011 and 0.193 ± 0.010, respectively [12].

Also, in view of the approximate nature of the wave functions used, we had to scale the calculated excitation energies by the ratio of the experimental and theoretical IEs to make the theoretical transition energies more realistic. In this way, individual EA cross sections may not be accurate, but we are confident that the sum of such cross sections will be realistic both in the range of excitation energies and magnitudes.

For an ion, excitation cross sections must be calculated using the Coulomb Born (CB) approximation, which gives nonvanishing threshold values, in contrast to neutral targets whose threshold values must vanish. The CB cross sections require hundreds of thousands, if not millions, of angular coefficients because the incident electron before and after the collision is represented by partial-waves. For the open-shell configurations of Mo^{+}, the old MCDF code was quickly saturated and we were able to calculate the necessary partial waves only for $\ell \leq 10$. This in turn limited the reliability of the resulting CB cross sections to incident energies near the excitation thresholds.

To overcome this restriction, we relied on the fact that a CB excitation cross section merges to the plane-wave Born (PWB) excitation cross section calculated with the same wave functions at high T. We used the high-T PWB cross sections and the CB threshold values to derive an analytic expression for the entire range of T. The Bethe approximation expresses a high-T PWB cross section in terms of three parameters α, β and γ, which are ab initio constants calculated from the initial and final state wave functions [13]:

$$\sigma_{\mathrm{Bethe}}(T) = \frac{4\pi a_0^2}{T/R}\left[\alpha \ln\left(\frac{T}{R}\right) + \beta + \frac{\gamma R}{T}\right]. \tag{6}$$

We modified the value of γ so that σ_{Bethe} matches the calculated CB cross section at the threshold. In other words, the constant γ' is chosen to satisfy the following equation:

$$\sigma_{\mathrm{exc}}(T = E) = \frac{4\pi a_0^2}{E/R}\left[\alpha \ln\left(\frac{E}{R}\right) + \beta + \frac{\gamma' R}{E}\right]. \tag{7}$$

Finally, the CB cross sections obtained from Eq. (7) were reduced using the E scaling, Eq. (5).

The sums of the cross sections for these selected, "significant" autoionizing excitations for the ground level and metastable Mo^{+} are included in Table A.2 with the total ionization cross sections, i.e., sum of the direct and indirect ionization cross sections. The total ionization cross sections for the ground level and metastable Mo^{+} are compared to experimental data on single ionization, i.e., $Mo^{+} \rightarrow Mo^{2+}$, in Fig. 1. The experimental data near the threshold clearly indicate that a substantial fraction of the target ions were metastable. The shape of both experimental data beyond the cross section peak and that of the present theory disagree. This may be an indication that the "correct" EA cross sections may drop off

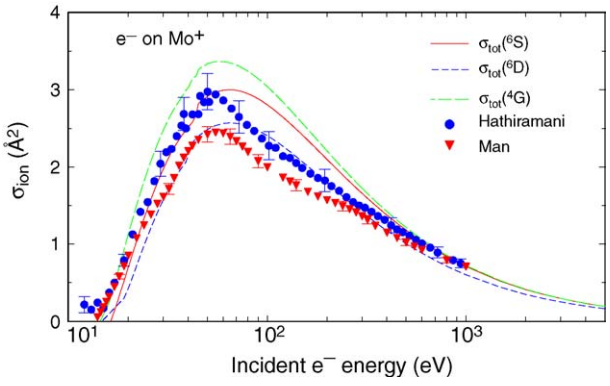

Fig. 1. Comparison of the present work to experimental single ionization cross sections of Mo^{+}. Solid curve, total ionization cross section for the ground level $^6S_{5/2}$; medium dashed curve, total ionization cross section for the metastable level $^6D_{5/2}$; long dashed curve, total ionization cross section for the metastable level $^4G_{5/2}$; triangles, experimental data by Man et al. [6]; circles, experimental data by Hathiramani et al. [7].

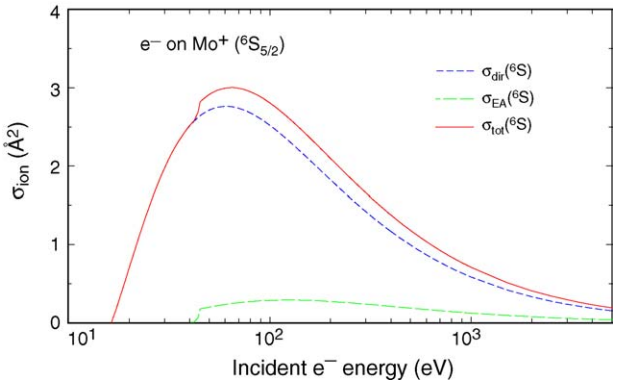

Fig. 2. Theoretical single ionization cross sections of Mo^+ in the $^6G_{5/2}$ ground level. Medium dashed curve, direct ionization cross section; long dashed curve, excitation–autoionization cross section; solid curve, total ionization cross section.

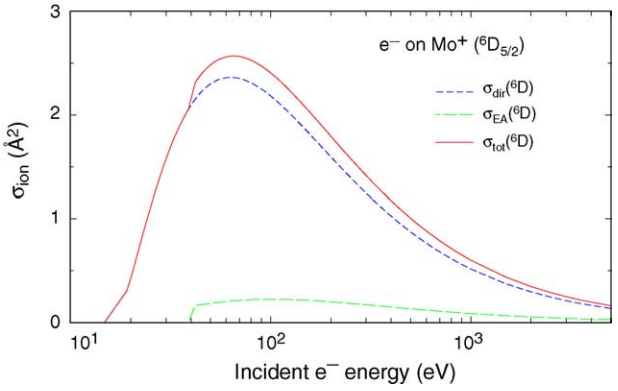

Fig. 3. Theoretical single ionization cross sections of Mo^+ in the $^6D_{5/2}$ metastable level. Medium dashed curve, direct ionization cross section; long dashed curve, excitation–autoionization; solid curve, total ionization cross section.

rapidly after the threshold, unlike the curves for EA cross sections shown in Figs. 2–4. The direct ionization, EA, and total ionization cross sections for the ground and two metastable levels of Mo^+ are presented in Figs. 2–4.

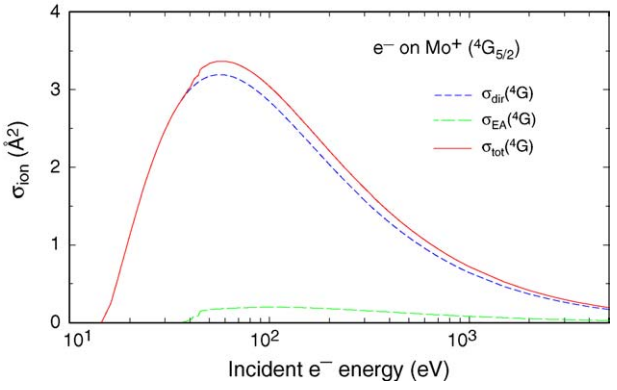

Fig. 4. Theoretical single ionization cross sections of Mo^+ in the $^4G_{5/2}$ metastable level. Medium dashed curve, direct ionization cross section; long dashed curve, excitation–autoionization; solid curve, total ionization cross section.

4. Cross sections for Mo

For the neutral Mo atom, we calculated ionization cross sections for the ground level, $4d^55s\ ^7S_3$, and two metastable levels, $4d^55s\ ^5S_2$ and $4d^45s^2\ ^5D_2$.

4.1. Direct ionization

The direct ionization cross sections were calculated using Eqs. (1) and (2). Among the levels in the second metastable term, $^5D_2$ was chosen to match the J value of the first metastable level, which simplified some computational steps. Again, we recall that the cross sections for the members of a fine-structure multiplet are very similar, almost independent of J.

The 5s electron is ionized in the case of the ground level and the first metastable Mo producing Mo^+ in the ground level, $4d^56\ ^5S_{5/2}$, while the second metastable level produces a metastable Mo^+ in the $4d^45s\ ^6D$ term. From the NIST database [11], we find that the IE of the ground level $^6S_3$ is 7.09243 eV, and the IE of the first metastable level $^5S_2$ is $7.09243 - 1.33510 = 5.75733$ eV. For the second metastable level, we assumed that the neutral Mo is in the $^5D_2$ level and the metastable Mo^+ produced is in the $4d^45s\ ^6D_{5/2}$ level, making the IE of the metastable Mo to be $7.09243 - 1.42016 + 1.53955 = 7.21182$ eV. Note that this is slightly higher than the IE of the ground level.

The orbital parameters for the ground and metastable levels of Mo are listed in Table A.3. The direct ionization cross sections for the ground and two metastable levels are listed in Table A.4.

4.2. Indirect ionization

"Significant" contributions to the indirect ionization of Mo come from the EA of 5s, 4d → 5p and 4p → 4d, 5s excitations. As in the case of Mo^+, we retained only $E1$-allowed excitations with $f > 0.05$. Although there are no 4d → 4f excitations with $f > 0.05$, some autoionizing excitations correspond to the 5s → 5p and 4p → 5s excitations. In contrast, there are no significant contributions from the 5s → 5p and 4d → 5p, 4f excitations in Mo^+. Excitations of the type 4d → 5p significantly contribute to indirect ionization at low T for the metastable terms ^5S and ^5D, but not to the ground term ^7S. We included 13 excitations for the ionization of the ground level $^7S_3$, 25 excitations for the metastable level $^5S_2$, and 35 excitations for the metastable level $^5D_2$. Of the 17 strong ($f > 0.2$) excitations, two were $\Delta n = 1$ transitions, and three were spin-forbidden, again indicating the breakdown of LS coupling as in Mo^+. The sum of these autoionizing cross sections and the total ionization cross sections for each initial level are presented in Table A.4. The graphs of the direct, EA, and total ionization cross sections of Mo in the ground level and the two metastable levels are shown in Figs. 5–7.

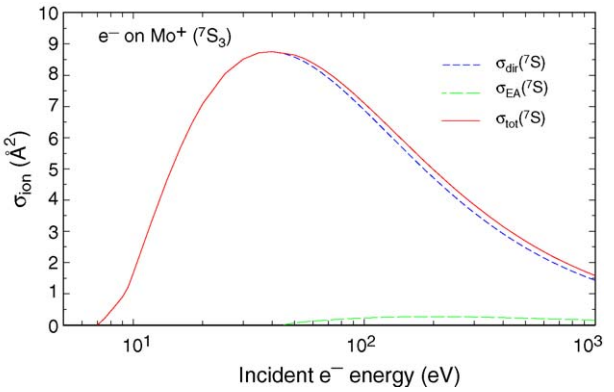

Fig. 5. Theoretical single ionization cross sections of Mo in the $^7S_3$ ground level. Medium dashed curve, direct ionisation cross section; long dashed curve, excitation–autoionization cross section; solid curve, total ionization cross section.

As was done for Mo^+, we used configuration average radial functions to calculate 4p and 4d excited states to be included in the indirect ionization. The excitation energies of the selected levels were scaled by the ratio of the calculated and known experimental IEs to make the excitation energies more realistic. As was explained in Section 2.2, *BE*-scaled PWB cross sections (see Eq. (4)) were used to calculate the autoionization cross sections. In reality, because of their moderately high excitation energies (∼40 eV), some of the 4p-excited levels may decay by photoemission, and hence not produce an ion. The evaluation of the branching ratios for photoemission versus autoionization is a major theoretical undertaking beyond the scope of the present study. We have assumed that all 4p hole states decay by autoionization since autoionization is still a dominant process for excitation energies much less than 100 eV.

There are no experimental data on neutral Mo for comparison. However, theoretical ionization cross section calculated by Badnell et al. [8] at low T using the distorted-wave Born (DWB) approximation is compared to our total ionization cross sections of the ground level and metastable Mo in Fig. 8. Although the DWB cross sections are for direct ionization only, the shape of the DWB cross sections indicates that the DWB cross sections would be about one half of our cross sections for direct ionization at the peak. The DWB cross sections calculated by Pindzola et al. [7] for Mo^+ and by Badnell et al. [8] for Mo have two versions depending on the effective potential used for the incident electron, the "prior" and "post" approximations. The "prior" version produces a broad peak near the threshold that more than doubles the cross section, but the "prior" version eventually comes down close in magnitude to the "post" version at high T.

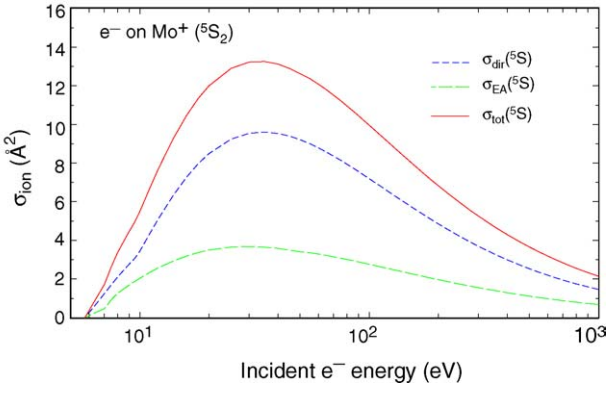

Fig. 6. Theoretical single ionization cross sections of Mo in the $^5S_2$ metastable level. Medium dashed curve, direct ionization cross section; long dashed curve, excitation–autoionization cross section; solid curve, total ionization cross section.

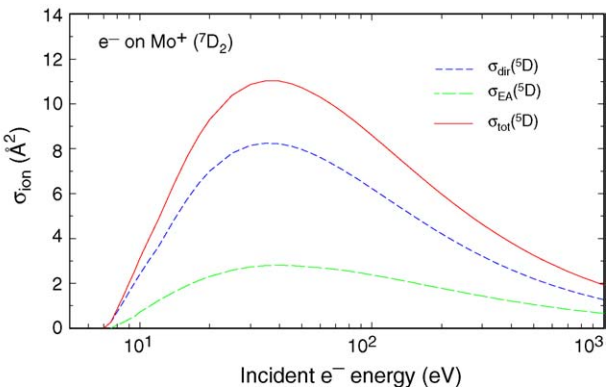

Fig. 7. Theoretical single ionization cross sections of Mo in the $^5D_2$ metastable level. Medium dashed curve, direct ionization cross section; long dashed curve, excitation–autoionization cross section; solid curve, total ionization cross section.

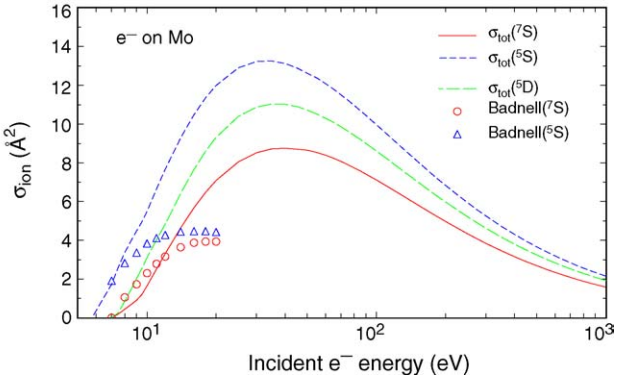

Fig. 8. Comparison of the present work to the distorted-wave Born cross sections of Mo by Badnell et al. [8]. Solid curve, total single ionization cross section for the $^7S_3$ ground level; medium dashed curve, total single ionization cross section for the $^5S_2$ metastable level; long dashed curve, total single ionization cross section for the $^5D_2$ metastable level; circles, direct ionization cross section by Badnell et al. [8] using the distorted-wave Born approximation ("post" version) for the $^7S_3$ ground level; triangles, direct ionization cross section by Badnell et al. [8] using the distorted- wave Born approximation ("post" version) for the $^5S_2$ metastable level.

5. Conclusions

The combination of the BEB model for the direct ionization and the *BE* and *E* scaling of the plane-wave and Coulomb

Born cross sections for the indirect ionization through EA offers a practical and reliable total ionization cross section for Mo^+ as is clearly demonstrated by the experimental data shown in Fig. 1. We can now safely answer the questions raised in Section 1 concerning the extension of the theoretical methods tested only on light, neutral atoms or atoms with simple valence structures to heavy atoms with complex valence structures and their singly charged ions. Relativistic effects manifest themselves through noticeable cross sections for spin-forbidden excitations. Different metastable Mo and Mo^+ have distinct cross sections, and the peak cross sections for metastable Mo are larger than that for the ground level Mo by 25–50%. For Mo^+, the peak cross section for one of the metastable terms is lower than the peak cross section for the ground level Mo^+. In contrast, peak cross sections for the ground levels of all atoms studied previously by the same theoretical method were lower than the peak cross sections of matching metastable atoms. The good agreement between our theoretical results and experimental data on Mo^+ supports the method and criteria we have used to select "significant" EA cross sections from the vast number of autoionizing excitations. Finally, we also conclude that we can use the same theoretical models for both neutral Mo and Mo^+.

In contrast to our results, the conventional distorted-wave Born cross section calculated by Pindzola et al. [7] for direct ionisation of Mo^+ is about a factor of two higher than the experiments. Adding EA cross sections will make the disagreement worse. Although the DWB cross sections ("post" version) for the neutral Mo calculated by Badnell et al. [8] agree with our results at low $T < 15$ eV, their cross sections stay flat beyond $T \sim 15$ eV, indicating that their peak values will be substantially lower than ours.

Indirect processes dominated by the 5s- and 4d-excited levels increase the ionization cross sections of metastable Mo atoms by almost 25–40%. For the ground level Mo, indirect processes increase the ionization cross section by only about 5%, because most of the 5s- and 4d-excited levels with high spins are bound, and only 4p-excited levels contribute to autoionization. For Mo^+, only 4p-excited levels contribute to autoionization.

Although the present method requires less computational effort than most conventional theories (except for the Lotz formula), the amount of work is by no means trivial. The fact that the present theory can use without significant modifications cross sections calculated with relativistic wave functions offer decisive advantage when we apply our theory to heavy atoms. The good agreement of the present theory to experimental results on Mo^+ provides optimism that we not only can trust our cross sections for the neutral Mo but also we can produce reliable ionization cross sections for W and W^+. At present, there is no reliable alternative for calculating cross sections for heavy neutral atoms and their lightly charged ions with complex valence shell structures.

Acknowledgements

We are deeply indebted to Dr. Jean-Paul Desclaux and Dr. Paul Indelicato for providing us with their multiconfiguration Dirac–Fock code, which was indispensable in obtaining the necessary wave functions and collision cross sections. The work at NIST was supported in part by the Office of Fusion Sciences of the United States Department of Energy. The work at KAERI was supported in part by the Fusion Plasma Users Group Support Program of the Korea Basic Science Institute. One of us (YKK) would like to thank Dr. Shiyang Zou and Dr. Takako Kato of the National Institute for Fusion Science for their assistance in the initial stage of this work.

Appendix A

Table A.1
Orbital binding energy B, kinetic energy U, and electron occupation number N for the ground and two metastable levels of Mo^+

Orbital[a]	$^6S_{5/2}$			$^6D_{5/2}$			$^4G_{5/2}$		
	B (eV)	U (eV)	N[b]	B (eV)	U (eV)	N[b]	B (eV)	U (eV)	N[b]
1s	20127.41	24587.76	2	20131.40	24587.64	2	20127.91	24587.75	2
2s	2922.891	5090.390	2	2927.144	5090.508	2	2923.421	5090.397	2
2p*	2679.924	5051.729	2	2684.154	5051.619	2	2680.468	5051.700	2
2p	2572.668	4780.666	4	2576.855	4780.676	4	2573.189	4780.690	4
3s	535.1317	1353.543	2	539.3737	1354.120	2	535.6441	1353.603	2
3p*	441.2083	1288.644	2	445.4146	1288.915	2	441.7276	1288.731	2
3p	422.8818	1229.673	4	427.0659	1229.862	4	423.3899	1229.722	4
3d*	257.8275	1100.087	4	262.0236	1100.149	4	258.3646	1100.155	4
3d	254.3661	1084.348	6	258.4626	1083.953	6	254.8536	1084.056	6
4s	85.7001	279.4591	2	89.6364	284.9249	2	86.1324	279.8973	2
4p*	56.5079	233.9864	2	60.2401	238.2429	2	57.0341	234.3853	2
4p	53.7376	222.7542	4	57.0282	227.4976	4	54.0636	223.3618	4
4d*	16.3499	113.1985	2.09183	19.4610	122.3572	1.91241	16.0594	113.1023	2.19043
4d	16.2962	111.1550	2.90817	19.0881	119.7213	2.08759	14.4118	109.1476	2.80957
5s				14.7567	36.9422	1			

[a] *Notation*: $nl^* = nl_{j=l-1/2}$, $nl = nl_{j=l+1/2}$.

[b] The non-integer occupation numbers for the $4d_{3/2}$ and $4d_{5/2}$ electrons resulted from distributing the single nonrelativistic configuration $4d^5$ or $4d^4$ among the combinations of relativistic configurations containing $4d_{3/2}$ and $4d_{5/2}$ electrons.

Table A.2
Cross sections of Mo^+ in the ground and metastable levels for direct ionization σ_{dir}, excitation–autoionization σ_{EA}, and total ionization σ_{tot} resulting in the production of Mo^{2+} in its ground term as a function of incident electron energy T

T (eV)	$^6S_{5/2}$			$^6D_{5/2}$			$^4G_{5/2}$		
	σ_{dir}	σ_{EA}	σ_{tot}	σ_{dir}	σ_{EA}	σ_{tot}	σ_{dir}	σ_{EA}	σ_{tot}
14.412							0		0
14.5							0.0131		0.0131
14.757				0		0	0.0514		0.0514
15				0.0183		0.0183	0.0882		0.0882
16				0.0937		0.0937	0.2406		0.2406
16.296	0		0	0.1157		0.1157	0.3060		0.3060
18	0.3255		0.3255	0.2348		0.2348	0.7039		0.7039
20	0.7015		0.7015	0.4264		0.4264	1.1315		1.1315
25	1.4648		1.4648	1.1020		1.1020	1.9539		1.9539
30	1.9763		1.9763	1.5777		1.5777	2.4795		2.4795
40	2.5142	0.0036	2.5178	2.0953	0.0677	2.1630	3.0023	0.0243	3.0266
50	2.7150	0.1996	2.9146	2.3006	0.1839	2.4845	3.1727	0.1651	3.3378
60	2.7625	0.2337	2.9962	2.3612	0.2015	2.5626	3.1888	0.1781	3.3669
70	2.7375	0.2563	2.9939	2.3522	0.2122	2.5645	3.1346	0.1865	3.3211
80	2.6777	0.2712	2.9489	2.3091	0.2185	2.5276	3.0485	0.1917	3.2402
90	2.6017	0.2808	2.8825	2.2496	0.2217	2.4713	2.9494	0.1944	3.1438
100	2.5194	0.2865	2.8059	2.1829	0.2228	2.4057	2.8464	0.1956	3.0420
125	2.3137	0.2908	2.6046	2.0118	0.2204	2.2322	2.5985	0.1940	2.7925
150	2.1271	0.2874	2.4145	1.8540	0.2142	2.0682	2.3795	0.1892	2.5687
175	1.9645	0.2805	2.2450	1.7152	0.2066	1.9218	2.1913	0.1831	2.3744
200	1.8237	0.2722	2.0959	1.5945	0.1987	1.7931	2.0299	0.1766	2.2065
250	1.5952	0.2545	1.8497	1.3974	0.1835	1.5809	1.7701	0.1638	1.9339
300	1.4189	0.2378	1.6567	1.2448	0.1700	1.4148	1.5713	0.1523	1.7235
400	1.1661	0.2092	1.3753	1.0250	0.1479	1.1729	1.2877	0.1332	1.4210
500	0.9934	0.1867	1.1801	0.8744	0.1311	1.0055	1.0951	0.1185	1.2136
600	0.8678	0.1688	1.0365	0.7645	0.1180	0.8824	0.9554	0.1069	1.0623
700	0.7720	0.1542	0.9262	0.6806	0.1074	0.7880	0.8492	0.0975	0.9467
800	0.6964	0.1422	0.8386	0.6143	0.0987	0.7130	0.7655	0.0898	0.8553
900	0.6351	0.1321	0.7672	0.5605	0.0915	0.6520	0.6977	0.0833	0.7811
1000	0.5844	0.1234	0.7078	0.5160	0.0853	0.6013	0.6417	0.0778	0.7195
1500	0.4214	0.0939	0.5152	0.3726	0.0645	0.4371	0.4620	0.0591	0.5210
2000	0.3324	0.0765	0.4088	0.2941	0.0524	0.3465	0.3641	0.0481	0.4121
3000	0.2365	0.0567	0.2931	0.2095	0.0387	0.2481	0.2588	0.0356	0.2943
4000	0.1851	0.0455	0.2306	0.1641	0.0310	0.1950	0.2024	0.0285	0.2310
5000	0.1528	0.0383	0.1911	0.1355	0.0260	0.1615	0.1670	0.0240	0.1910

All cross sections are in $Å^2$.

Table A.3
Orbital binding energy B, kinetic energy U, and electron occupation number N for the ground and metastable levels of Mo

Orbital[a]	$^7S_3$			$^5D_2$			$^5D_2$		
	B (eV)	U (eV)	N[b]	B (eV)	U (eV)	N[b]	B (eV)	U (eV)	N[b]
1s	20120.54	24587.73	2	20120.85	24587.75	2	20124.27	24587.64	2
2s	2916.126	5090.488	2	2916.362	5090.422	2	2920.052	5090.54	2
2p*	2673.129	5051.717	2	2673.384	5051.716	2	2677.058	5051.586	2
2p	2565.876	4780.654	4	2566.127	4780.657	4	2569.746	4780.672	4
3s	528.3625	1353.86	2	528.6118	1353.647	2	532.2969	1354.228	2
3p*	434.4033	1288.703	2	434.6737	1288.630	2	438.3256	1288.897	2
3p	416.0767	1229.726	4	416.3465	1229.652	4	419.9711	1229.819	4
3d*	251.0006	1100.046	4	251.2886	1100.054	4	254.9422	1100.177	4
3d	247.5433	1084.327	6	247.8243	1084.302	6	251.3539	1083.855	6
4s	78.8720	281.9674	2	79.2025	279.1892	2	82.6101	284.5194	2
4p*	49.5046	234.5370	2	49.9756	233.8045	2	53.2473	237.8078	2
4p	46.7453	223.1774	4	47.1928	222.5275	4	49.9245	227.1294	4
4d*	9.3582	107.8245	2.08149	9.7313	111.7360	2.10143	12.3112	120.9355	1.98009
4d	9.2799	105.5788	2.91851	9.6553	109.7995	2.89857	11.8903	118.2601	2.01991
5s	7.0924	25.5912	1	5.7573	13.8724	1	7.2118	25.8657	2

[a] *Notation*: $nl^* = nl_{j=l-1/2}$, $nl = nl_{j=l+1/2}$.

[b] The non-integer occupation numbers for the $4d_{3/2}$ and $4d_{5/2}$ electrons resulted from distributing the single nonrelativistic configuration $4d^5$ or $4d^4$ among the combinations of relativistic configurations containing $4d_{3/2}$ and $4d_{5/2}$ electrons.

Table A.4
Cross sections of Mo in the ground and metastable levels for direct ionization σ_{dir}, excitation–autoionization σ_{EA}, and total ionization σ_{tot} resulting in the production of ground level Mo^+ ($4d^5 {}^6S$) from the Mo $^7S_3$ and $^5S_2$ levels and the production of the metastable Mo^+ ($4d^4\ 5s {}^6D$) from the Mo $^5D_2$ level as a function of incident electron energy T in eV

T (eV)	$^7S_3$			$^5S_2$			$^5D_2$		
	σ_{dir}	σ_{EA}	σ_{tot}	σ_{dir}	σ_{EA}	σ_{tot}	σ_{dir}	σ_{EA}	σ_{tot}
5.7573				0	0	0			
6.5				0.7633	0.3068	1.0702			
7				1.2524	0.4728	1.7252			
7.5	0.1972		0.1972	1.7015	0.9291	2.6305	0.2648		0.2648
8	0.4407		0.4407	2.1058	1.2616	3.3673	0.7301	0.1321	0.8622
8.5	0.6764		0.6764	2.4655	1.4924	3.9579	1.1848	0.2544	1.4392
9	0.8992		0.8992	2.7833	1.6973	4.4806	1.6172	0.4018	2.0190
10	1.6490		1.6490	3.4472	2.0479	5.4952	2.3951	0.7164	3.1115
12	3.3037		3.3037	5.0867	2.5752	7.6620	3.6071	1.2197	4.8268
14	4.6404		4.6404	6.3454	2.9412	9.2866	4.8080	1.6041	6.4120
16	5.6779		5.6779	7.2838	3.1977	10.4815	5.7557	1.8993	7.6550
18	6.4747		6.4747	7.9777	3.3774	11.3551	6.4705	2.1267	8.5972
20	7.0847		7.0847	8.4888	3.5019	11.9907	7.0047	2.3021	9.3068
25	8.0495		8.0495	9.2378	3.6584	12.8962	7.8063	2.5838	10.3901
30	8.5207		8.5207	9.5389	3.6882	13.2271	8.1512	2.7252	10.8763
40	8.7545		8.7545	9.5339	3.5864	13.1202	8.2209	2.8013	11.0222
50	8.5838	0.0654	8.6492	9.2092	3.4111	12.6204	7.9646	2.7562	10.7208
60	8.2707	0.1193	8.3899	8.7907	3.2969	12.0877	7.6105	2.6904	10.3009
70	7.9143	0.1564	8.0707	8.3586	3.1538	11.5124	7.2387	2.6186	9.8573
80	7.5554	0.1839	7.7393	7.9429	3.0159	10.9588	6.8790	2.5366	9.4157
90	7.2109	0.2048	7.4157	7.5545	2.8869	10.4414	6.5422	2.4539	8.9961
100	6.8873	0.2207	7.1080	7.1960	2.7675	9.9635	6.2311	2.3730	8.6041
125	6.1767	0.2461	6.4227	6.4232	2.5087	8.9318	5.5605	2.1871	7.7475
150	5.5925	0.2586	5.8511	5.7981	2.2969	8.0950	5.0185	2.0266	7.0451
175	5.1095	0.2639	5.3734	5.2862	2.1211	7.4073	4.5749	1.8889	6.4638
200	4.7052	0.2650	4.9702	4.8604	1.9731	6.8334	4.2062	1.7701	5.9763
250	4.0686	0.2604	4.3290	4.1939	1.7370	5.9309	3.6294	1.5759	5.2053
300	3.5906	0.2519	3.8425	3.6960	1.5567	5.2528	3.1989	1.4244	4.6232
400	2.9202	0.2321	3.1522	3.0007	1.2978	4.2985	2.5977	1.2019	3.7996
500	2.4709	0.2133	2.6842	2.5364	1.1194	3.6558	2.1964	1.0454	3.2418
600	2.1478	0.1969	2.3447	2.2031	0.9882	3.1913	1.9083	0.9286	2.8369
700	1.9035	0.1827	2.0862	1.9516	0.8870	2.8386	1.6908	0.8376	2.5284
800	1.7119	0.1705	1.8824	1.7545	0.8065	2.5610	1.5204	0.7646	2.2849
900	1.5574	0.1599	1.7173	1.5957	0.7406	2.3363	1.3830	0.7044	2.0874
1000	1.4300	0.1506	1.5806	1.4648	0.6856	2.1503	1.2698	0.6539	1.9237
1500	1.0237	0.1176	1.1413	1.0478	0.5058	1.5536	0.9090	0.4891	1.3980
2000	0.8039	0.0973	0.9012	0.8225	0.4052	1.2277	0.7138	0.3939	1.1077
3000	0.5689	0.0733	0.6422	0.5817	0.2946	0.8763	0.5052	0.2881	0.7933
4000	0.4438	0.0595	0.5032	0.4537	0.2340	0.6877	0.3942	0.2298	0.6240
5000	0.3655	0.0504	0.4159	0.3736	0.1954	0.5690	0.3247	0.1925	0.5172

All cross sections are in $Å^2$.

References

[1] Y.-K. Kim, M.E. Rudd, Phys. Rev. A 50 (1994) 3954.
[2] Y.-K. Kim, Phys. Rev. A 64 (2001) 032713.
[3] Y.-K. Kim, Phys. Rev. A 65 (2002) 022705.
[4] Y.-K. Kim, P.M. Stone, Phys. Rev. A 64 (2001) 052707.
[5] Y.-K. Kim, J.P. Desclaux, Phys. Rev. A 66 (2002) 012708.
[6] K.F. Man, A.C.H. Smith, M.F.A. Harrison, J. Phys. B 20 (1987) 1351.
[7] D. Hathiramani, K. Aichele, G. Hofmann, M. Steidl, M. Stenke, R. Völpel, E. Salzborn, M.S. Pindzola, J.A. Shaw, D.C. Griffin, N.R. Badnell, Phys. Rev. A 54 (1996) 587.
[8] N.R. Badnell, T.W. Gorczyca, M.S. Pindzola, H.P. Sommers, J. Phys. B 29 (1996) 3683.
[9] See http://physics.nist.gov/ionxsec.
[10] J.P. Desclaux, P. Indelicato, See http://dirac.spectro.jussieu.fr/mcdf.
[11] NIST Atomic Spectroscopic Database (http://physics. nist. gov/PhyRefData).
[12] W.F. Chan, G. Cooper, X. Guo, G.R. Burton, C.E. Brion, Phys. Rev. A 46 (1992) 149.
[13] Y.-K. Kim, M. Inokuti, Phys. Rev. A 3 (1971) 665.